Quantum-classical correspondence in integrable systems

Yiqiang Zhao(赵义强)[1] and Biao Wu(吴飙)[1, 2, 3, *]

[1] International Center for Quantum Materials, School of Physics, Peking University, Beijing 100871, China
[2] Collaborative Innovation Center of Quantum Matter, Beijing 100871, China
[3] Wilczek Quantum Center, Department of Physics and Astronomy, Shanghai Jiao Tong University, Shanghai 200240, China

(Dated: January 22, 2018)

We find that in integrable quantum systems there exist two time scales. One is the Ehrenfest time below which the system is classical; the other is the quantum revival time beyond which the system is fully quantum. In between, the quantum system can be well approximated by classical ensemble distribution in phase space. These results can be summarized in a diagram which we call Ehrenfest diagram. We derive an analytical expression for Ehrenfest time, which is proportional to $\hbar^{-1/2}$. According to our formula, the Ehrenfest time for the solar-earth system is about 10^{26} times of the age of the solar system. We also find an analytical expression for the quantum revival time, which is proportional to $\hbar^{-1}$. Both time scales involve $\omega(I)$, the classical frequency as a function of classical action. Our results are numerically illustrated with a simple one dimensional integrable model. We show that similar results exist for Bose gases, which may provide an experimental platform for measuring these time scales.

I. INTRODUCTION

A quantum system is expected to become classical in the limit $\hbar \to 0$. However, how this exactly happens is highly non-trivial and has been studied intensively in the field of quantum chaos [1]. The issue of quantum-classical correspondence was noticed as early as in 1927 by Ehrenfest. For a particle with mass m moving in a potential $V(x)$, Ehrenfest demonstrated that the expectation values of the particle's position and momentum follow Newton-like equations [2]

$$\frac{d}{dt}\langle\hat{x}\rangle = \frac{\langle\hat{p}\rangle}{m} \quad (1)$$

$$\frac{d}{dt}\langle\hat{p}\rangle = -\langle\frac{dV(\hat{x})}{d\hat{x}}\rangle \quad (2)$$

where $\langle\cdot\rangle$ is the expectation value of the operator. These two equations are now known as Ehrenfest theorem, which offers a hint on how quantum and classical dynamics may be related. In particular, when the wave function is narrow enough and/or the potential $V(x)$ varies gradually in space, we approximately have $\langle\frac{dV(\hat{x})}{d\hat{x}}\rangle \approx \frac{dV(\langle\hat{x}\rangle)}{d\langle\hat{x}\rangle}$. This means that the evolution of expectation values of position and momentum would follow exactly the Newton's equation of motion. However, an initially well-localized wave packet will spread, and the expectation values of its position and momentum will eventually deviate from the classical dynamics when the width of the wave packet is no longer small. Ehrenfest time $\tau_\hbar$ is the time scale when such a quantum-classical correspondence breaks down [3–12].

In this work we study systematically the quantum-classical correspondence in integrable systems. We find that beside Ehrenfest time there exist another time scale when quantum revival occurs. This time scale is quantum revival time T_r [13]. It is similar to the time scale in quantum kicked rotor beyond which the true quantum phenomenon, dynamical localization or quantum resonance, occurs [14]. Between Ehrenfest time $\tau_\hbar$ and quantum revival time T_r, a quantum integrable system can be well approximated by classical ensemble distribution in phase space.

Furthermore, we are able to derive analytical expression for both Ehrenfest time $\tau_\hbar$ and quantum revival time T_r, both of which are intimately related to $\omega(I)$, the classical frequency as a function of classical action. We find that $\tau_\hbar \propto \hbar^{-1/2}$ and $T_r \propto \hbar^{-1}$.

For many specific systems, we find that the Ehrenfest time has a simple form $\tau_\hbar = cT_c(I/\hbar)^{1/2}$, where T_c is the period of a classical motion, I is the corresponding action, and c is a dimensionless constant of order one. Our results are applied to many concrete systems. Generally, for systems which we usually regard as quantum systems, their Ehrenfest times are short; for systems which we usually consider as classical systems, their Ehrenfest times are long. For example, for a hydrogen atom in the ground state, we have $\tau_\hbar = 0.5T_c$; for the earth orbiting around the sun, we have $\tau_\hbar = 2.3\times10^{36}T_c$ while the age of the solar system is only 0.5×10^9T_c. Therefore, Ehrenfest time may be used as an indicator whether we should treat a given system as quantum or classical.

In the end we consider an integrable system of Bose gas for which its effective Planck constant is $1/N$ [15], where N is the total number of the particle. When N is small, the Bose gas is quantum and when N is large it is well approximated by the mean-filed theory [16]. We also find two time scales, the Ehrenfest time scales with N as $N^{1/2}$ and the quantum revival time scales linearly with N. As N can be changed in an experiment, Bose gas offers a potential platform where the scalings of Ehrenfest time and quantum revival time with the Planck constant may

*Electronic address: wubiao@pku.edu.cn

be verified experimentally.

II. EHRENFEST TIME

Before we present our general results, it is illuminating to look at a concrete system with numerical simulation.

A. numerical results

We consider the following one dimensional system

$$H = \frac{p^2}{2m} + V(x) \tag{3}$$

where m is the mass of the particle and $V(x) = m\omega_0^2 x^2 + m^2\omega_0^3 x^4/\hbar$. To numerically investigate how Ehrenfest time scales with the Planck constant, we set the Planck constant in the Schrödinger equation as $\tilde{\hbar} = \hbar_\epsilon \hbar$, where the dimensionless constant $\hbar_\epsilon$ is varied. In our numerical calculation, we use $\sqrt{\hbar/(m\omega_0)}$ as unit of length, $\sqrt{\hbar m\omega_0}$ as unit of momentum, $\hbar\omega_0$ as unit of energy, and $1/\omega_0$ as unit of time. In this unit system, $V(x) = x^2 + x^4$.

We compare numerically the quantum and classical dynamics of this system. For a given classical initial condition x_0, p_0, we construct the following Gaussian wave packet as the initial state for the quantum dynamics,

$$\psi(x) = \frac{1}{(2\pi\sigma_x^2)^{1/4}} \exp\left\{-\frac{(x-x_0)^2}{4\sigma_x^2} + \frac{ip_0(x-x_0)}{\hbar_\epsilon}\right\}, \tag{4}$$

where $\sigma_x = \sqrt{\hbar_\epsilon/2}$. The quantum expectation value $\langle x(t)\rangle$ and the classical trajectory $x_c(t)$ are compared in Fig. 1(a). As expected, they match each other for an initial short period of time and then start to deviate. We find that the difference $|\langle x(t)\rangle - x_c(t)|$ oscillates and its peaks can be approximated by function $y = a(1-e^{-bt^2})$, as shown in the inset of Fig. 1(b). The Ehrenfest time is extracted from these numerical results as $\tau_\hbar = \sqrt{1/b}$. When $\hbar_\epsilon$ is varied, $\tau_\hbar$ varies. Their relation is shown in Fig. 1(b), which clearly shows $\tau_\hbar \propto \hbar^{-1/2}$.

In addition, we follow Ref. [17] and compare the quantum dynamics to its corresponding classical ensemble evolution. We use the Wigner function of the Gaussian wave packet in Eq.(4) as the initial distribution for a classical ensemble

$$\rho_c(x,p) = \frac{1}{\pi\hbar_\epsilon} \exp\left\{-\frac{(x-x_0)^2}{2\sigma_x^2} - \frac{(p-p_0)^2}{2\sigma_p^2}\right\}. \tag{5}$$

where $\sigma_x = \sigma_p = \sqrt{\hbar_\epsilon/2}$. We use $\bar{x}_c$ as the classical ensemble average of x. The agreement between the quantum expectation value $\langle x(t)\rangle$ and $\bar{x}_c(t)$ is almost perfect for a short period of time as shown in Fig. 1(a). Such an excellent agreement goes beyond just the averaged value and exists even in phase space. To plot the quantum dynamics in phase space, we use the method

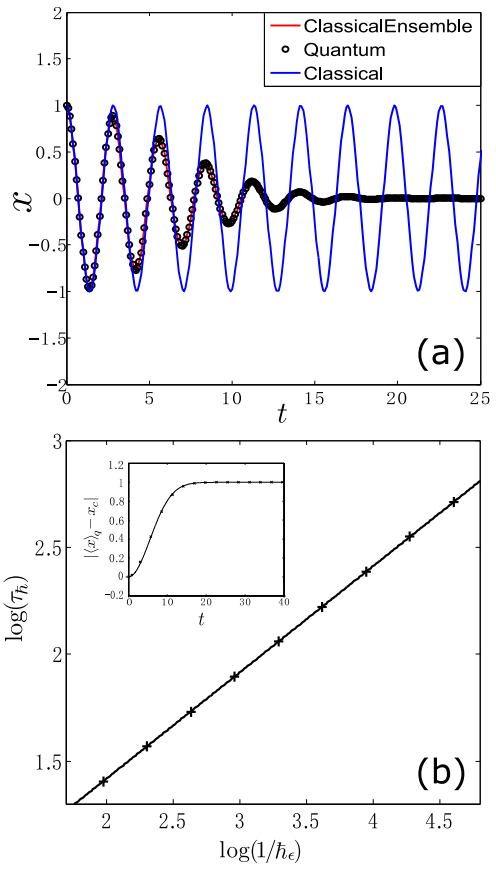

FIG. 1: (color online) (a) The time evolutions of a classical particle $x_c(t)$, its corresponding quantum expectation value $\langle x(t)\rangle$, and the corresponding classical ensemble average $\bar{x}_c(t)$. $x_0 = 1$, $p_0 = 0$, and $\hbar_\epsilon = 0.03$. (b) Relationship between between $\tau_\hbar$ and $1/\hbar_\epsilon$, which can be fit by function $y = 0.5x + 0.42$. The inset is a typical fit curve of the evolution of the peaks of the difference between classical value and quantum expectation value. The unit of length is $\sqrt{\hbar/(m\omega_0)}$ and the unit of time is $1/\omega_0$.

in Refs.[18, 19] to project wave function unitarily onto quantum phase space. Roughly, the classical phase space is divided into Planck cells and each Planck cell is assigned a Wannier function; these Wannier function form a complete orthonormal basis which is used for the unitary projection. The results are plotted in Fig. 2, where we see that the agreement is excellent within Ehrenfest time and it begins to break only after $t = 26$.

B. General analysis

The numerical results above also indicate that a single-particle classical trajectory deviates from its corresponding classical ensemble dynamics (see Fig. 1(a)), which was already noticed in Ref.[17]. This fact, together with the perfect agreement between quantum dynamics and classical ensemble dynamics within Ehrenfest time, im-

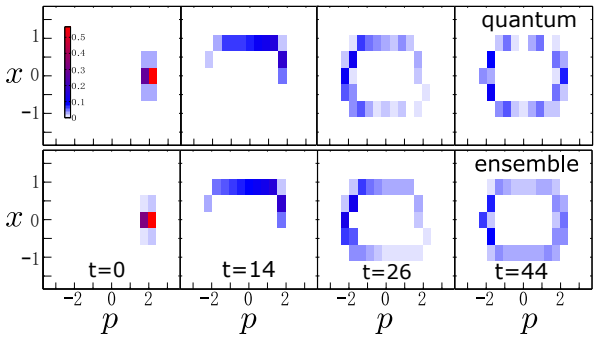

FIG. 2: (color online) Quantum dynamics (upper row) and classical ensemble dynamics (lower row) in phase space. The classical ensemble distribution is coarse-grained to Planck cells. For this case, $\tau_\hbar \approx 26$. $(x_0 = 0, p_0 = 2)$ and $\hbar_\epsilon = 0.03$. The unit of length is $\sqrt{\hbar/(m\omega_0)}$, the unit of time $1/\omega_0$, and the unit of momentum $\sqrt{\hbar m\omega_0}$.

plies that Ehrenfest time $\tau_\hbar$ is solely caused by the width of a quantum wave packet that has a lower limit set by the uncertainty relation. We exploit it to derive an analytical expression for Ehrenfest time.

We consider a classical ensemble distribution that satisfies the uncertainty relation, such as the one in Eq.(4). The evolution of this classical ensemble is governed by Liouville equation, which is totally classical and irrelevant of $\hbar$. The only factor related to $\hbar$ is the fluctuations of position and momentum in this ensemble distribution which are limited by the uncertainty principle.

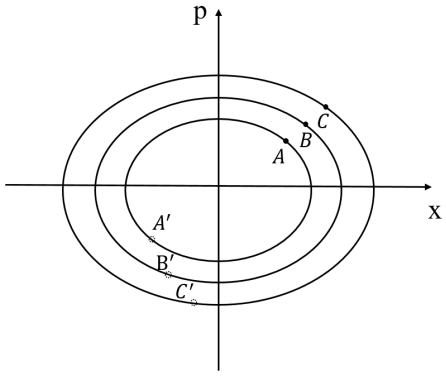

FIG. 3: A typical phase space for one dimensional integrable system. Closed curves are energy contours. In general, the oscillation frequencies on different curves are different. So, the three points A, B, and C , initially close to each other, will disperse over time due to different fequencies.

We choose three points A, B, and C in the phase space such that they initially differ from each other by δp in momentum and δx in position (see Fig.3). In particular, B is the averaged point of A and C. As long as the system is not a harmonic oscillator, these three points have different angular velocities. As time goes by, the average of A and C will differ significantly from B and the correspondence between classical ensemble and classical single particle will break down. When we choose $\delta x \cdot \delta p \sim \hbar$, such a breakdown time is just Ehrenfest time $\tau_\hbar$.

We define $\tau_\hbar$ as the time when the angular difference of A and C is 2π. We thus have

$$\tau_\hbar = \frac{2\pi}{|\omega_A - \omega_C|} \tag{6}$$

$$\approx \frac{2\pi\omega(I)}{|\omega'(I)| \cdot |\partial H/\partial x \cdot \delta x + \partial H/\partial p \cdot \delta p|} \tag{7}$$

where ω is the angular velocity and I is the action. Note that all these quantities $\omega'(I)$, $\partial H/\partial x, \partial H/\partial p$ and $\omega(I)$ are classical and independent of $\hbar$. The Planck constant comes in only through the uncertainty relation that requires that $\delta x \sim \delta p \propto \hbar^{1/2}$. So, we have

$$\tau_\hbar \propto \hbar^{-1/2}\,. \tag{8}$$

There is no need to worry about the possibility $\omega'(I) = 0$ in Eq.(7) as it is the result of truncation of the Taylor expansion of $|\omega_A - \omega_C|$ to the first order. If $\omega'(I) = 0$, one just needs to expand it further to the second order. In this case, we would have $\tau_\hbar \propto \hbar^{-1}$. One could continue this expansion until some order becomes non-zero. If all orders of derivative of $\omega(I)$ vanish, the system must be a harmonic oscillator for which $\tau_\hbar$ is indeed infinite.

For chaotic systems, it is well accepted that [3–9] that Ehrenfest time $\tau_\hbar = \frac{c}{\gamma}\ln\frac{A}{\hbar}$, where γ is the Lyapunov index of the chaotic system, A is a typical action, and c is a dimensionless constant of order one. However, there is some confusion over Ehrenfest time in integrable systems. Although it is generally believed that for integrable systems Ehrenfest time scales with the Planck constant as $\tau_\hbar \propto \hbar^{-\alpha}$ [20], it is not clear in literature what α is. It was indicated in Ref. [11] that $\alpha = 1$. However, it is shown in some specific cases that $\alpha = 1/2$ [20, 21]. Berry and Balazs found that $\alpha = 2/3$ [7]. Our work clarifies this issue and shows analytically $\alpha = 1/2$. Note that Ehrenfest time is intrinsic to the system and is independent of initial conditions. It can be understood as the time scale that a classical ensemble distribution in phase space develops structures finer than Planck cell.

C. Examples

We now apply the above result to a couple of examples to get a sense how big or small the Ehrenfest time can become in typical macroscopic and microscopic situations. The first example is a particle of mass m in a one dimensional box of length a. Through some simple calculations we have

$$\tau_\hbar = T_c\sqrt{\frac{2I}{\hbar}} \tag{9}$$

where $I = pa/\pi$ is the action and $T_c = 2am/p$ is the classical period with p being the momentum of the particle.

Here we consider two typical scenarios, one macroscopic and one microscopic. Imagine that a macroscopic ball moves in a box with $m = 1\text{g}$, $a = 1\text{m}$, $v = 1\text{m/s}$. The Ehrenfest time for this system is then $\tau_\hbar = 2.4 \times 10^{15} T_c$. Naturally, classical mechanics is enough to describe such a system. For the microscopic scenario, we consider a ultracold ^{87}Rb atom moving in a optical well [22], where $m = 1.5 \times 10^{-25}\text{kg}$, $v = 10^{-3}\text{m/s}$ (estimated under condition $T = 10^{-8}\text{K}$), and $a = 10^{-7}\text{m}$ (roughly the wavelength of light). The Ehrenfest time for this case is $\tau_\hbar = 0.8 T_c$. So ultracold atoms must be described by quantum mechanics. This example shows that Ehrenfest time is a good indicator whether a system should be regarded as quantum or classical.

The second example is a system with the inverse square law of force, whose Hamiltonian is

$$H = \frac{p_r^2}{2m} + \frac{L^2}{2mr^2} - \frac{k}{r} \tag{10}$$

where m is the mass of the object, r is the distance to the center, p_r is the radial momentum, and L is the angular momentum. With canonical transformation, we have

$$H = -\frac{mk^2}{2}\frac{1}{(I+L)^2} \tag{11}$$

where I is the action variable of the system other than L. To simplify the calculations, we choose a special initial condition $r = \frac{L^2}{mk}$, and the variances of the wave packet are $\delta r = \sqrt{\hbar/(2m\omega)}$, $\delta p_r = \sqrt{m\omega\hbar/2}$, $\delta\theta = \frac{1}{r}\sqrt{\hbar/(2m\omega)}$, and $\delta L = r\sqrt{m\omega\hbar/2}$. With some simple calculations we have

$$\tau_\hbar = \frac{\sqrt{2}}{3}\frac{T_c}{\sqrt{\frac{\hbar[(I+L)^2-L^2]}{L^2(I+L)}} + \frac{L}{I+L}\sqrt{\frac{\hbar}{L}}} \tag{12}$$

For the sun-earth system, as the motion is approximate circular motion, we have $I \approx 0$ and $L = 2.7 \times 10^{39} J \cdot s$. So, we hace $\tau_\hbar = 2.3 \times 10^{36}$ years while the age of the solar system is just 5×10^9 years. For a hydrogen atom in it ground state, as $L = \hbar$ we have $\tau_\hbar = 0.5 T_c$. This is clearly consistent with our daily experientce that we do not need to worry about the quantum effects in the orbits of the solar planets while we have to describe hydrogen atom with quantum mechanics.

III. QUANTUM REVIVAL TIME

Ehrenfest time gives us the time scale when the quantum dynamics of a single particle deviates from its classical trajectory. However, as shown in Fig. 1, if one compares the dynamics of a quantum wave packet to an ensemble of classical orbits, the quantum-classical correspondence can last much longer. This phenomenon of course has been noticed a long time ago [17]. In this section, we investigate how long the quantum-classical correspondence can last in this sense. We find that for integrable systems such a time scale is set by quantum revival [13] and scales with the Planck constant as $\hbar^{-1}$.

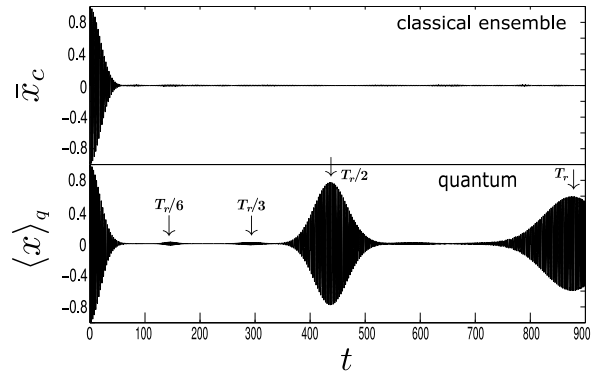

FIG. 4: (Upper) Time evolution of the classical ensemble average $\bar{x}_c(t)$; (Lower) time evolution of the quantum expectation value $\langle x(t) \rangle$. T_r is the quantum revival time. $(x_0 = 0, p_0 = 2)$ and $\hbar_\epsilon = 0.03$. The unit of length is $\sqrt{\hbar/(m\omega_0)}$ and the unit of time $1/\omega_0$.

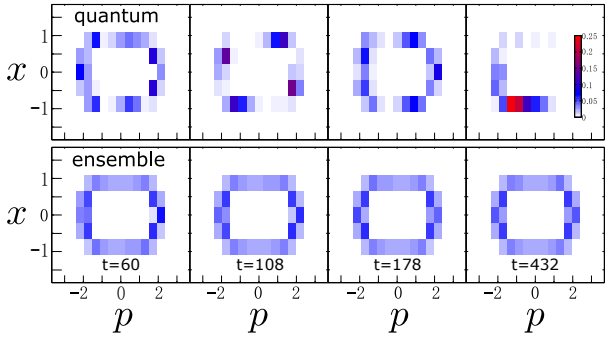

FIG. 5: (color online) Quantum dynamics (upper row) and classical ensemble dynamics (lower row) in phase space. The classical ensemble distribution is coarse-grained to Planck cells. For this case, $T_r \approx 864$. $(x_0 = 0, p_0 = 2)$ and $\hbar_\epsilon = 0.03$. The unit of length is $\sqrt{\hbar/(m\omega_0)}$, the unit of time $1/\omega_0$, and the unit of momentum $\sqrt{\hbar m\omega_0}$.

A. Numerical results

We further study numerically the quantum dynamic and its corresponding classical ensemble dynamics for much longer times. They are compared in term of the averaged position (see Fig. 4) and also in phase space (see Fig. 5). If one is only interested in the dynamics of the wave packet center, the quantum and classical ensemble results match each other very well for a very long time, up to $t > 300$ according to Fig. 4. After that, around $t \approx 430$, while the classical average $\bar{x}_c(t)$ remains around zero, the quantum expectation $\langle x(t) \rangle$ almost fully recovers its original value, which is known as quantum revival.

This quantum revival occurs again when the evolution time is doubled.

However, if one is interested in more dynamical details, the time scale of agreement is shortened by a few fractions. According to Fig. 5, after $t = \tau_\hbar \approx 26$, both are no longer localized. However, the quantum distribution always has more structures while the classical ensemble distribution is rather uniformly distributed within the energy shell. In particular, at certain times, one observes that the quantum distribution will cluster around a few centers, a phenominon known as fractional quantum revival [13]. At $t = 432$, which is half of the quantum revival time, we see that the quantum distribution becomes localized again.

B. Analytical results

The numerical results above show that quantum dynamics and its corresponding classical ensemble dynamics begin to deviate from each other significantly when quantum revival occurs . In this subsection, we derive an analytic formula for quantum revival time. We follow the method in Ref. [13] but with a significant modification by introducing action variables. For a general one dimensional integral system, its classical Hamiltonian can always be written as $H(I)$, where I is the action of the system. As a result, its classical energy is also a function of the action $E(I)$ and so is the classical frequency $\omega(I) = \partial E(I)/\partial I$ [23]. We expand the quantum wave packet in terms of the system's energy eigenstates and its dynamics is then given by

$$\psi(t) = \sum_n c_n e^{-iE_n t/\hbar}\phi_n(x)\,, \tag{13}$$

where $\phi_n(x)$ is the nth eigenstate and E_n is its corresponding energy eigenvalue. The coefficients c_n's are determined by the initial condition. We assume that $|c_m|^2$ is the largest and expand the eigenvalue around E_m as follows

$$E_n = E_m + \omega(I_m)(I_n - I_m) + \frac{\omega'(I_m)}{2}(I_n - I_m)^2 + ... \tag{14}$$

where I_n is the action corresponding to E_n via $E(I)$. According to the Bohr-Sommerfeld quantization rule [24], we have

$$I_n - I_m = (n-m)\hbar\,. \tag{15}$$

So, the quantum phases can be written as

$$\begin{aligned} &\exp\left[-i(E_n - E_m)t/\hbar\right] \\ =\ &\exp\left[-2\pi i(n-m)\frac{t}{T_c} - 2\pi i(n-m)^2\frac{t}{T_r} + ...\right] \end{aligned} \tag{16}$$

where $T_c = 2\pi/\omega(I_m)$ and

$$T_r = \frac{4\pi}{\omega'(I_m)\hbar}\,. \tag{17}$$

As T_r contains $\hbar$ in its denominator, it is clear that $T_r \gg T_c$. With this in mind, we can envision from Eq.(16) how the quantum wave packet will evolve in time. For an initial short interval of time, the wave packet will oscillate with period T_c but with a decaying amplitude due to the second-order and other higher order terms. When the evolution time approaches T_r, the second-order terms become multiples of 2π and, as a result, the wave packet recovers most of its original shape. How much it can recover depends on the third and higher order terms and other factors. Before T_r, there can be fractional quantum revivals that occur at $t = pT_r/q(p,\, q$ are positive integers); they are characterized by a superposition of several localized wave packets [13]. This is exactly what we have observed in Fig. 5.

From the above discussion, we find that the quantum revival time T_r scales with the Planck constant as $T_r \propto \frac{1}{\hbar}$. For the two examples mentioned in Sec. II C, according to Eq. (17), we have

$$T_{r1} = T_c\frac{2I}{\hbar}\,, \tag{18}$$

and

$$T_{r2} = \frac{2}{3}T_c\frac{I+L}{\hbar}\,, \tag{19}$$

respectively.

We note that the Bohr-Sommerfeld quantization rule is only an approximation; Eq.(15) should be corrected to $I_n - I_m = (n-m)\hbar + \delta_e$. For the above analysis to be correct, the condition $\omega(I_m)\delta_e \ll \frac{\omega'(I_m)}{2}(n-m)^2\hbar^2$ should be satisfied. δ_e also affects how much the quantum wave packet can recover its original shape at T_r.

IV. BOSE GASES

It is well known that the relationship between quantum and mean field descriptions of Bose gases is essentially quantum-classical correspondence [15, 16] with $1/N$(N is the total number of bosons) serves as effective Planck constant. Our results above can be straightforwardly applied to any system of Bose gas which is integrable as it was done for chaotic Bose system in Ref. [16]. We illustrate this with a two-site Bose-Hubbard model as an example, whose Hamiltonian is

$$\hat{H} = -\frac{\nu}{2}(\hat{a}^\dagger\hat{b} + \hat{a}\hat{b}^\dagger) + \frac{c}{2N}(\hat{a}^\dagger\hat{a}^\dagger\hat{a}\hat{a} + \hat{b}^\dagger\hat{b}^\dagger\hat{b}\hat{b}) \tag{20}$$

where c is the strength of interaction and ν is the tunneling parameter. In our numerical calculation, we use ν as unit of energy, $\hbar/\nu$ as unit of time. When the particle number N is large, this system can be well approximated by the following mean field model

$$H_{\rm mf} = -\frac{\nu}{2}(a^*b + ab^*) + \frac{c}{2}(|a|^4 + |b|^4)\,. \tag{21}$$

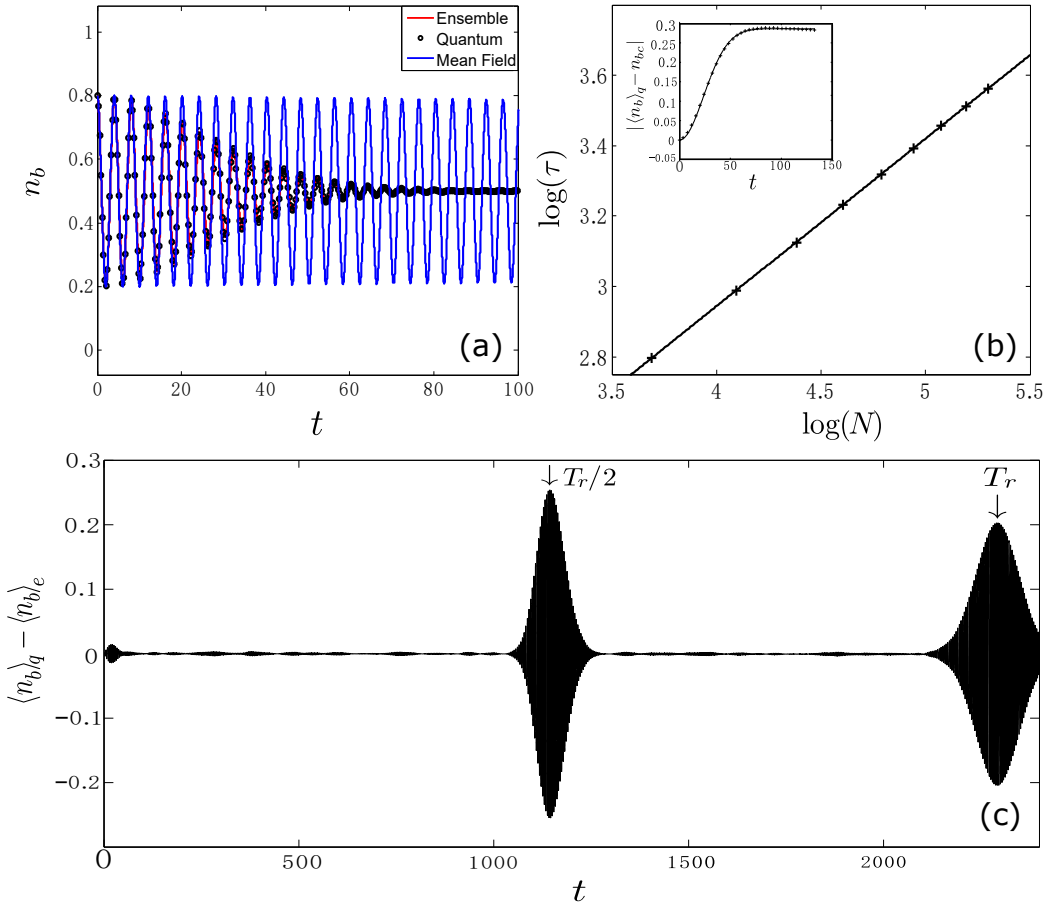

FIG. 6: (color online) (a) The time evolution of the averaged probability of the system is in state b according to three different dynamics: quantum, mean-field, and mean field ensemble. (b) Ehrenfest time as a function of number of particles N, which can be fit by $y = 0.48x + 1$. (c) The evolution of difference between quantum expectation value and mean field ensemble average of occupation probability at state b. $N = 200$, $c/\nu = 2$. The unit of time is $\hbar/\nu$

.

Owing to the particle number conservation, $|a|^2 + |b|^2 = 1$, and the overall phase is trivial, we can introduce a pair of conjugate variables s and θ, where $s = |b|^2$, $\theta = \theta_b - \theta_a$ with θ_b and θ_a being the phases of complex numbers a and b. The mean field model is clearly a classical one dimensional integrable system.

In the above discussion of quantum-classical correspondence of a single particle, a point in the classical phase space corresponds to a Gaussian wave packet of minimal spread. For this Bose system, a mean field state $a = \alpha$, $b = \beta$ corresponds to a quantum coherent state$|\alpha, \beta\rangle$

$$|\alpha, \beta\rangle = \frac{1}{\sqrt{N!}}(\alpha a^\dagger + \beta b^\dagger)^N |0\rangle \,. \tag{22}$$

However, we need some effort to construct the corresponding mean field ensemble distribution $\rho(s, \theta)$. We expand the coherent state $|\alpha, \beta\rangle$ with Fock states $|n, N-n\rangle$, where n is the particle number at site a,

$$|\alpha, \beta\rangle = \sum_s \varphi_N(s)|N - Ns, Ns\rangle \,, \tag{23}$$

where

$$\varphi_N(s) = \sqrt{\frac{N!}{Ns!(N - Ns)!}}\alpha^{N-Ns}\beta^{Ns} \,. \tag{24}$$

and s ranges over $0/N, 1/N, ..., N/N$. $|\varphi_N(s)|^2$ can be regarded as a distribution of s. For this distribution, the average of s is $\bar{s} = |\beta|^2$ and its variance is

$$\Delta s = \frac{|\beta|\sqrt{(1 - |\beta|^2)}}{\sqrt{N}} \,. \tag{25}$$

As θ is the conjugate of s, its distribution can be obtained with a Fourier transform

$$\phi_N(\theta) = \frac{1}{\sqrt{N+1}} \sum_s \varphi_N(s) e^{-iNs\theta} \tag{26}$$

where θ takes the following discrete values: $2\pi\frac{1}{N+1}, 2\pi\frac{2}{N+1}, ..., 2\pi\frac{N+1}{N+1}$. Numerical results show that

$$\bar{\theta} \approx \theta_\beta - \theta_\alpha \,, \qquad \Delta\theta \approx \frac{1}{2\sqrt{N}|\beta|\sqrt{(1 - |\beta|^2)}} \,. \tag{27}$$

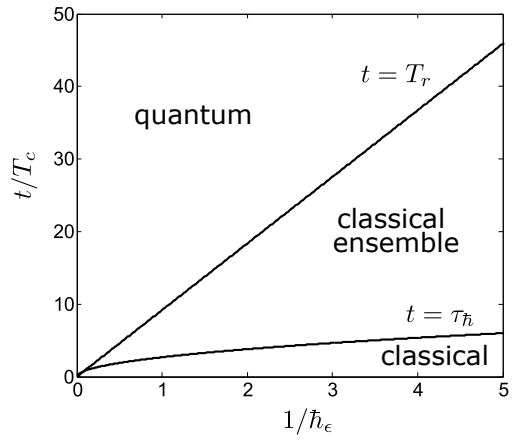

FIG. 7: Ehrenfest diagram. Two time scales, Ehrenfest time and quantum revival time, are plotted as functions $1/\hbar_\epsilon$. These two times scales mark up three regions: quantum, classical ensemble, and classical. $(x_0 = 0, p_0 = 2)$ is the initial condition for this figure.

So, $\Delta\theta$ and Δs satisfy the uncertainty relation:$\Delta\theta\Delta s \approx \frac{1}{2N}$. At the large N limit, $N \to +\infty$, both $|\varphi_N(s)|^2$ and $|\phi_N(\theta)|^2$ will approach Gaussian distribution. If we denote these two Gaussian distributions as $g_1(s)$ and $g_2(\theta)$, respectively, the mean-field ensemble distribution can be constructed as $\rho(s,\theta) = g_1(s)g_2(\theta)$. The three different dynamics, mean-field, mean-field ensemble, and quantum, are compared in Fig. 6. We find a very similar pattern as we found in Sections III and IV.

For quantum revival, we would need the Bohr-Sommerfeld quantization rule. How to implement this rule in the mean field theory of a Bose gas is discussed in Ref.[25, 26].

In conclusion, the breakdown of correspondence between quantum and mean field descriptions occurs at time $\tau_\hbar \propto N^{1/2}$, and the breakdown of correspondence between quantum and mean field ensemble occurs at time $T_r \propto N$. The Planck constant $\hbar$ can not be changed experimentally, but total number of bosons N can. Therefore, the Bose gases can be used to experimentally verify the results in this paper.

V. DISCUSSION AND CONCLUSION

In summary, we have shown that for a generic integrable system there exist two different time scales, Ehrenfest time $\tau_\hbar \propto \hbar^{-1/2}$ and and quantum revival time $T_r \propto \hbar^{-1}$. When they are plotted in Fig. 7, they mark up three different regions in the space spanned by $\hbar$ and dynamical evolution time t. In the classical region, a narrow quantum wave packet does not spread much and its center follows the classical particle trajectory. In the classical ensemble region, a quantum wave packet can be regarded as a classical ensemble distribution in phase space. In the quantum region, quantum revival occurs and the quantum dynamics can not even be approximated with classical ensemble.

We call Fig. 7 Ehrenfest diagram for two reasons. The first is to honor Ehrenfest for his pioneering work on quantum-classical correspondence [2]. The second and more important reason is that we expect the prominent feature, three different regions marked up by two different time scales, in Fig. 7 to be generic. Even for chaotic systems, this feature is expected to persist; the difference is that the Ehrenfest time becomes logarithmic and the quantum revival time will be replaced by other quantum times that scale with $\hbar$ differently. For example, for quantum kicked rotor, the second time is the time scale for dynamical localization or quantum resonance and it scales as $\hbar^{-2}$ [14]. We may call this second time scale quantum time. We note that this quantum time in our integrable systems is not Heisenberg time: as indicated in Eq.(16), the quantum revival comes from the second-order terms in the eigen-energy expansion.

It would be very interesting to see how this kind of Ehrenfest diagram evolves when a system changes from integrable to chaotic. It is not clear how Ehrenfest time changes from square root to logarithmic. For a chaotic system, the quantum revival time is likely exponentially long, so the quantum time in the chaotic system must have a different cause. It is not clear what the cause is or whether this cause may change from system to system.

Acknowledgments

We acknowledge helpful discussion with Yuan Fang on plotting Figs.2&5. This work was supported by the The National Key Research and Development Program of China (Grants No. 2017YFA0303302) and the National Natural Science Foundation of China (Grants No. 11334001 and No. 11429402).

[1] M. C. Gutzwiller, *Chaos in classical and quantum mechanics* (Springer, New York, 1990).
[2] P. Ehrenfest, Zeitschrift für Physik A Hadrons and Nuclei **45**, 455 (1927).
[3] G. P. Berman and G. M. Zaslavsky, Physica A: Statistical Mechanics and its Applications **91**, 450 (1978).
[4] G. M. Zaslavsky, Physics Reports **80**, 157 (1981).
[5] M. Combescure and D. Robert, Asymptotic Analysis **14**,

377 (1997).
[6] G. A. Hagedorn and A. Joye, in *Annales Henri Poincaré* (Springer, 2000), vol. 1, pp. 837–883.
[7] M. Berry, Journal of Physics A: Mathematical and General **12**, 625 (1979).
[8] P. Silvestrov and C. Beenakker, Physical Review E **65**, 035208 (2002).
[9] C. Tian, A. Kamenev, and A. Larkin, Phys. Rev. B **72**, 045108 (2005).
[10] D. R. Grempel, S. Fishman, and R. E. Prange, Phys. Rev. Lett. **53**, 1212 (1984).
[11] S. Fishman, D. R. Grempel, and R. E. Prange, Phys. Rev. A **36**, 289 (1987).
[12] Y.-C. Lai, E. Ott, and C. Grebogi, Phys. Lett. A **173**, 148 (1993).
[13] R. W. Robinett, Physics Reports **392**, 1 (2004).
[14] F. M. Izrailev, Phys. Rep. **196**, 299 (1990).
[15] L. G. Yaffe, Reviews of Modern Physics **54**, 407 (1982).
[16] X. Han and B. Wu, Physical Review A **93**, 023621 (2016).
[17] L. Ballentine, Y. Yang, and J. Zibin, Physical review A **50**, 2854 (1994).
[18] X. Han and B. Wu, Physical Review E **91**, 062106 (2015).
[19] Y. Fang, F. Wu, and B. Wu, arXiv:1708.06507 (2017).
[20] G. P. Berman, E. N. Bulgakov, and D. D. Holm, *Crossover-time in quantum boson and spin systems*, vol. 21 (Springer Science & Business Media, 2008).
[21] G. Berman, A. Iomin, and G. Zaslavsky, Physica D: Nonlinear Phenomena **4**, 113 (1981).
[22] F. Dalfovo, S. Giorgini, L. P. Pitaevskii, and S. Stringari, Rev. Mod. Phys. **71**, 463 (1999).
[23] V. I. Arnold, *Mathematical Methods of Classical Mechanics* (Springer-Verlag, New York, 1978).
[24] A. Messiah, *Quantum Mechanics* (Dover, New York, 1999).
[25] B. Wu and J. Liu, Phys. Rev. Lett. **96**, 020405 (2006).
[26] X. Luo, Q. Xie, and B. Wu, Phys. Rev. A **77**, 053601 (2008).